that at any temperature examined the former value is larger than the latter by a factor which is beyond the errors in extrapolated s_L. Literally taken, this means that the ΔG for an adjacent pair of BLG and CBL residues is lower than the sum of those for BLG and CBL residues. This conclusion is consistent with a recent finding by Nishioka[25,26] that the helix stability of BLG–CBL–BLG block copolymers in the same solvent system can be explained if a certain number of CBL residues located on the block boundaries are given a value of s_L larger than that of the other CBL residues. In contrast, in their theory of random copolypeptides, Scheraga and collaborators[13,14] assumed that the statistical weight matrix associated with a given residue would be independent of the kind of its nearest neighbor residues. This assumption is equivalent to the approximation basic to eq 7 that the free-energy differences are additive. As far as the BLG–CBL pair in DCA–EDC mixtures is concerned, such an assumption is not likely to hold due to the conformational induction. However, it may be premature to conclude this to be a general trend, because this effect may vary with different pairs of residues and also with different arrangement of residues. We are now engaged in its study, with a series of sequential polypeptides consisting of BLG and CBL residues.

Acknowledgments. The authors wish to thank Professor H. Fujita for valuable discussion and criticisms.

References and Notes

(1) On leave of absence from the Department of Polymer Science and Technology, School of Engineering, Inha University, Inchon, Korea.
(2) P. Urnes and P. Doty, *Adv. Protein Chem.*, **16**, 401 (1961).
(3) G. D. Fasman, "Poly-α-Amino Acids", G. D. Fasman, Ed., Marcel Dekker, New York, N.Y., 1967, p 559.
(4) A. Teramoto and H. Fujita, *Adv. Polym. Sci.*, **18**, 65 (1975).
(5) A. Teramoto and H. Fujita, *J. Macromol. Sci., Rev. Macromol. Chem.*, **15**, 165 (1976).
(6) P. Doty, J. H. Bradbury, and A. M. Holtzer, *J. Am. Chem. Soc.*, **78**, 947 (1956).
(7) T. Matsumoto and A. Teramoto, *Biopolymers*, **13**, 1347 (1974).
(8) M. Matsuoka, T. Norisuye, A. Teramoto, and H. Fujita, *Biopolymers*, **12**, 1515 (1973).
(9) K. Nakamoto, H. Suga, S. Seki, A. Teramoto, T. Norisuye, and H. Fujita, *Macromolecules*, **7**, 784 (1974).
(10) I. Omura, A. Teramoto, and H. Fujita, *Macromolecules*, **8**, 284 (1975).
(11) T. Hayashi, S. Emi, and A. Nakajima, *Polymer*, **16**, 396 (1975).
(12) B. J. Johnson, *J. Pharm. Sci.*, **63**, 313 (1974).
(13) P. H. von Dreele, D. Poland, and H. A. Scheraga, *Macromolecules*, **4**, 396 (1971).
(14) H. A. Scheraga, *Adv. Org. Chem. Phys.*, **6**, 103 (1968); *Chem. Rev.*, **71**, 195 (1971).
(15) I. Omura, D. C. Lee, S. Itou, A. Teramoto, and H. Fujita, *Polymer*, **17**, 847 (1976), Part I of this series.
(16) N. Sayama, K. Kida, T. Norisuye, A. Teramoto, and H. Fujita, *Polym. J.*, **3**, 538 (1972).
(17) N. Nishioka, A. Maekawa, and A. Teramoto, *Biopolymers*, in press.
(18) A. Nakajima and T. Hayashi, *Bull. Inst. Chem. Res., Kyoto Univ.*, **50**, 303 (1972).
(19) A. Roig, F. G. Blanco, and M. Cortijo, *Biopolymers*, **10**, 329 (1971).
(20) A. Weissberger, E. S. Proskauer, J. A. Riddick, and E. E. Toops, Jr., Ed., "Organic Solvents", Interscience, New York, N.Y., 1955.
(21) T. Norisuye, M. Matsuoka, A. Teramoto, and H. Fujita, *Polym. J.*, **1**, 691 (1970).
(22) D. Poland and H. A. Scheraga, "Theory of Helix–Coil Transition in Biopolymers", Academic Press, New York, N.Y., 1970.
(23) K. Okita, A. Teramoto, and H. Fujita, *Biopolymers*, **9**, 717 (1970).
(24) J. Applequist, *J. Chem. Phys.*, **38**, 934 (1963).
(25) N. Nishioka, Ph.D. Thesis, Osaka University, 1976.
(26) N. Nishioka and A. Teramoto, in preparation.

Vibrational Analysis of Peptides, Polypeptides, and Proteins. 3. α-Poly(L-alanine) †

J. F. Rabolt, W. H. Moore, and S. Krimm*

Harrison M. Randall Laboratory of Physics and Biophysics Research Division, Institute of Science and Technology, University of Michigan, Ann Arbor, Michigan 48109.
Received May 23, 1977

ABSTRACT: Starting with a force field transferred from our earlier studies on β-polypeptides, we have calculated the optically active normal vibration frequencies of α-helical poly(L-alanine) and poly(L-alanine-*N*-*d*). The 47/13 helical structure was used, and all atoms were included. Only small modifications to the force field were required, and most of these could be justified. The analysis indicates that amide II′ is in Fermi resonance with one component of CH_3 asymmetric bend, thus leading to a small modification of C–N and C=O stretching force constants. The agreement between calculated and observed Raman and infrared bands is quite good. This has encouraged us to calculate the influence of small structural changes on the spectrum as a means of explaining the observed effects of temperature changes.

In the two previous papers in this series[1,2] we have developed a detailed force field for β-polypeptides and applied this force field to the analysis of the antiparallel chain-rippled sheet structure of poly(glycine I) [$(GlyI)_n$] and to the antiparallel chain-pleated sheet structures of poly(L-alanine) [$(Ala)_n$] and poly(L-alanylglycine) [$(Ala\text{-}Gly)_n$]. In order that vibrational spectroscopy be a useful tool in studying the conformation of peptide systems, it is important to know how this force field can be extended to structures other than the β sheets. We have, therefore, undertaken the analysis of the vibrational spectrum of α-helical $(Ala)_n$. In studying the effects of deuteration on the IR spectrum and of temperature on the IR and Raman spectra, we have also tried to understand the influence of intramolecular forces on helical stability.

† Dedicated to the 80th Birthday of Maurice L. Huggins

The structure of α-$(Ala)_n$ has been studied by x-ray diffraction by many workers[3–6] and is known to be a right-handed α helix with 47 residues in 13 turns. These helices are hexagonally close packed in the crystal, the chain sense being random.[4]

There is an extensive literature on IR and Raman studies of α-$(Ala)_n$.[7–18] Almost all of these studies were carried out at room temperature, whereas our spectra were also obtained at low as well as high temperatures. Recently[17,19] Raman spectra of *N*-deuterated species have been reported. We have also obtained such spectra, as well as IR spectra, in the 1600–100-cm^{-1} region.

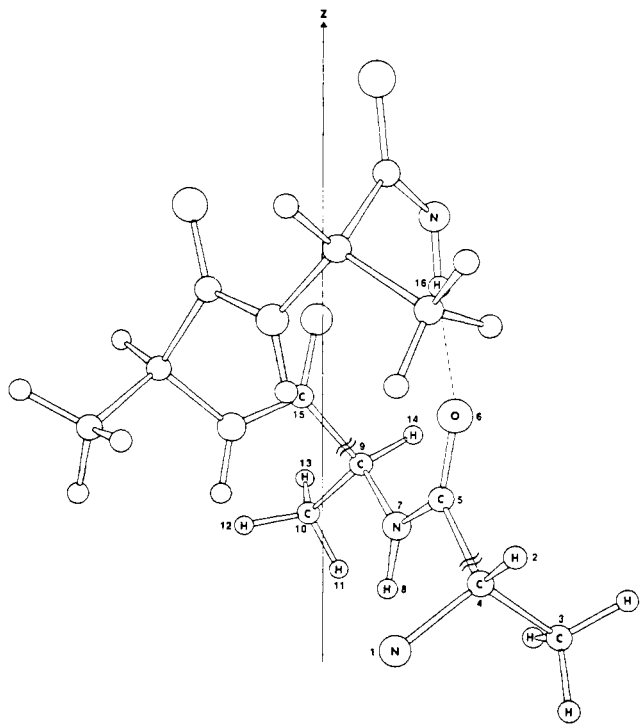

Figure 1. Portion of right-handed 47/13 helix of α-poly(L-alanine) with $\chi_1 = 0$.

Experimental Section

Samples of α-$(Ala)_n$ were obtained from Sigma Chemical Co. ($M_w \simeq 10\,000$, Lot 108B-2630) and Schwartz/Mann ($M_w \simeq 164\,000$, Lot X3319). Deuterated trifluoroacetic acid (TFA-*d*) was purchased from the Fisher Scientific Co.

Potassium bromide disks (13 mm) containing 5–10% $(Ala)_n$ by weight were pressed (at 10 000 psi) in an evacuated die and used for IR transmission measurements. Additional samples used in recording the far-IR and Raman spectra were prepared by placing 10 mg of $(Ala)_n$ in a die and exerting mild pressure (500 psi).

Progressively *N*-deuterated $(Ala)_n$ could be produced by suspending the finely powdered sample in D_2O and heating to 90–100 °C for 24 h. The solution was then placed in a vacuum oven and freeze dried. A small amount of material was then removed and mixed with KBr for IR measurements. The remaining sample was again dissolved in D_2O and this process was repeated. It was found that even after five repetitions of this procedure the $(Ala)_n$ was not completely *N*-deuterated.

A small amount of as-received material was dissolved in TFA-*d* in a closed container and allowed to sit for 30 min at room temperature. The solution was then placed in a vacuum oven and the TFA-*d* was allowed to evaporate at 25 °C. The IR spectrum of this material indicated that a significant number of NH groups had been deuterated. This procedure was again carried out with the remaining sample, and it was determined that a portion of the NH groups still remained undeuterated. Further attempts to obtain complete *N*-deuteration were unsuccessful.

Infrared spectra in the 4000–300-cm^{-1} region were recorded with a Perkin-Elmer 180 spectrometer equipped with an evacuated cold cell with KBr windows. This cell was modified to also permit obtaining high-temperature (150–200 °C) transmission measurements.

The low-frequency IR region of the spectrum was recorded with a Digilab FTS-16 fourier transform system. When using thick samples for the 100–30-cm^{-1} region it was found that a reasonably good signal-to-noise ratio could be obtained after 4000 scans.

Raman spectra were obtained with a spectrometer described previously.[20] A low-temperature cell was designed and constructed such that the samples could be fastened to a small copper block which was kept in constant contact with a reservoir of liquid nitrogen. The sample chamber was enclosed with a glass jacket and evacuated.

Structures. The standard α-helix structure used in the normal vibration calculation was that proposed by Brown and Trotter,[3] viz., a 47/13 helix with a *c*-axis periodicity of 70.3 Å. This corresponds to a rise per residue $h = 1.495$ Å, to torsional angles of $\phi = -54.44°$ and $\psi = -50.14°$, and to a rotation per residue about the helix axis of $t = 99.57°$. Bond lengths and angles were the same as in our work on β-$(Ala)_n$,[2] and as in that work the C^α–C^β torsion angle was set at $\chi_1 = 0°$. A portion of this helix is shown in Figure 1.

Table I
Force Constants Changed From β-$(Ala)_n$ to α-$(Ala)_n$

Force constant	Value α-$(Ala)_n$	Value β-$(Ala)_n$
Main chain		
f(N–H)	5.827	5.674
f(C=O)	9.700	9.720
f(C–N)	5.799	6.299
f(N–C^α–C)	1.095	0.595 (0.817)[a]
f(C–N–C^α)	1.090	0.787
f(C^α–N–H)	0.572	0.527
f(C–N–H)	0.572	0.527
f(N–H op)	0.171	0.129
f(H···O)	0.120	0.150
f(C^α–N, $NC^\alpha H^\alpha$)	0.517	0.217 (0.517)
f(N–H op, $NC^\alpha C$)	0.100	0.0
f(N–H op, $NC^\alpha C^\beta$)	0.150	0.0
f(N–C^α tor)		
f(C^α–C tor)	0.110	0.037
Side chain		
f(C^α–C^β)	4.587	4.387

[a] Values in parentheses are those used for $(GlyI)_n$.[1]

Previous observations on α-$(Ala)_n$ in the far IR at low temperatures[18] indicated a considerable change in intensity and a shift in frequency (3–5 cm^{-1}) of a number of bands located below 400 cm^{-1}. We have re-examined the spectrum in the 3800–400-cm^{-1} region at temperatures ranging from +150 to −150 °C and have found a number of additional bands that vary in intensity and frequency with temperature. In considering possible reasons for these changes, we investigated the effects of variations in structure on the vibrational frequencies. These were of three kinds: (1) changes in h, (2) changes in t, and (3) changes in χ_1. X-ray studies of *N*-deuterated α-poly(γ-benzyl L-glutamate)[21] had indicated that h could vary independently of t, and we therefore examined the effects of these two parameters separately. By varying χ_1 in 5° intervals from $\chi_1 = 0°$ (an H^β trans to H^α) we found that $H^\beta \cdots H^\alpha$ and $H^\beta \cdots O$ distances were maximized for $\chi_1 \simeq 20°$ (positive rotation is counterclockwise) when $h = 1.495$ Å but that smaller values of χ_1 gave acceptable distances when h was decreased or when t was decreased. It was therefore relevant to consider the influence of χ_1 on the vibrational spectrum, and calculations were therefore done for small changes in these three parameters.

Vibrational Analysis. The spectroscopically active modes of the 47/13 helix can be classified into A ($\delta = 0°$), E_1 ($\delta = 99.57°$), and E_2 ($\delta = 199.04°$) symmetry species, where δ is the phase difference between motions in adjacent residues. Both A and E_1 species are IR and Raman active, while the E_2 species is only Raman active. The A modes have parallel, and the E_1 modes perpendicular, dichroism in the IR. Group theoretical considerations show that there are 28 A modes, 29 E_1 modes, and 30 E_2 modes.[10]

The internal coordinates were defined as in the previous paper,[2] except that coordinates R_{12}, R_{31}, R_{32}, R_{39}, and R_{40} of Table IIB of ref 2 are not required for the helix. The local symmetry coordinates similarly follow the definitions given in Table III of the previous paper.[2]

We have shown[1,2] that transition dipole coupling is necessary to explain splittings that are observed in the amide I and amide II modes of β-polypeptides. Its effects have therefore been incorporated in the present calculation for the α helix. The amide I transition dipole was positioned as for β-$(Ala)_n$,[2] viz., with its center 0.868 Å from the carbon atom along the C → O direction and tilted 20° with respect to the C=O bond toward the N → C direction. The effective moment, $\Delta\mu_{eff} = (\partial\mu/\partial S)\Delta S$, was taken to be 0.305 D, 0.065 D less than that used for β-$(Ala)_n$. This decrease is consistent with the ratio of amide I intensities observed for the α helix[22] as compared to the β structure.[23] The amide II transition moment was also positioned as for β-$(Ala)_n$,[2] viz., with its center on the N–H bond and 0.6 Å from the H atom, and at an angle of 68° with the C=O bond toward N → C. The effective moment, $\Delta\mu_{eff}$, was taken to be 0.177 D, which is 0.092 D less than that used for β-$(Ala)_n$,[2] again based on the observed ratio of band intensities.[22,23] The transition dipole moments were summed over a radius of 35 Å, using the same formalism that was developed previously.[1] The contributions to the A, E_1, and E_2 species for amide I were −9.8, −5.5,

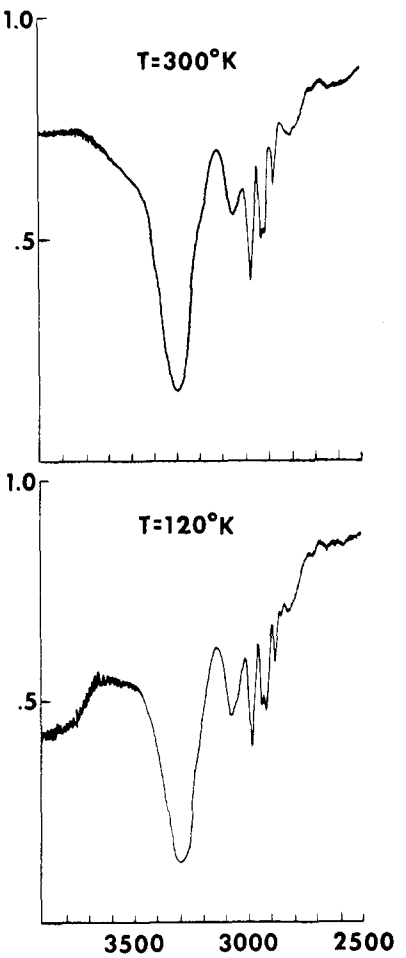

Figure 2. Infrared spectra of α-poly(L-alanine) in N–H and C–H stretching regions, at 300 and 120 K.

and −18.4 cm^{-1}, respectively, and for amide II they were −11.6, +6.2, and +4.5 cm^{-1}, respectively.

The initial force field used in the calculations was that derived from our previous studies on $(GlyI)_n$[1] and β-$(Ala)_n$.[2] Small changes in some force constants were then made in order to make obviously justifiable improvements in the fit to the spectra of α-$(Ala)_n$. The values of these force constants for the α helix are given in Table I. The analysis of α-(Ala-*N*-*d*)$_n$ showed that changes were also required in *f*(C=O) and *f*(C–N); these will be discussed below. The calculated frequencies of α-$(Ala)_n$ and α-(Ala-*N*-*d*)$_n$ are given in Tables II and III, respectively, and in each case assignments to observed bands are indicated.

Results and Discussion

(1) α-Poly(L-alanine). (a) N–H Stretching Region. Two bands appear in the region of N–H stretching, amide A near 3300 cm^{-1} and amide B near 3100 cm^{-1}, which arise from Fermi resonance between N–H stretching and overtones or combinations of amide II modes.[24] We have shown[2] that in β-$(Ala)_n$ amide B must have B_2 symmetry in order to interact with the unperturbed N–H stretching mode, and therefore most probably arises from a combination of amide II modes of B_1 and B_3 symmetries. In α-$(Ala)_n$ the amide B mode, at 3058 cm^{-1}, has parallel dichroism, and thus belongs to the A species. It therefore must arise from an overtone of amide II.

Using the observed intensity ratio, $I_R = I_B/I_A$, and the observed perturbed frequencies, ν_a and ν_b, it is possible to calculate[1,24] the unperturbed frequencies, ν_a^0 and ν_b^0. Infrared spectra of α-$(Ala)_n$ in this region, at 300 K and 120 K, are shown in Figure 2. Using the above method, the calculated unperturbed frequencies obtained from these spectra are given in Table IV. It is interesting to see that the predicted

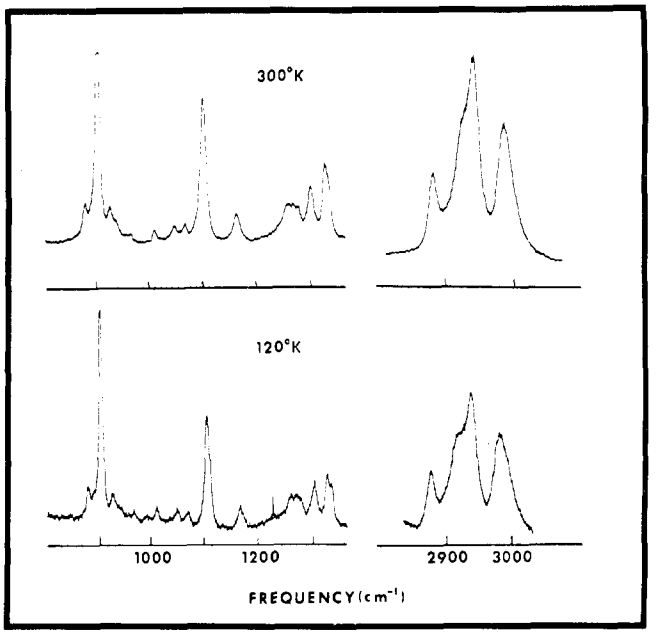

Figure 3. Raman spectra of α-poly(L-alanine) in 1400–800- and in 3000–2800-cm^{-1} regions, at 300 and 120 K.

amide II band agrees very well with the observed strong IR (E_1) mode and that its shift on going to low temperature is also in agreement with the observed shift.

The frequency of ν_a^0 at 300 K, namely 3279 cm^{-1}, is significantly higher than that for β-$(Ala)_n$,[2] namely 3242 cm^{-}. The force constant, *f*(N–H), is also higher, 5.827 compared to 5.674. This would correspond to a stronger N–H bond and therefore a weaker H···O bond, and it is satisfying to note that α-$(Ala)_n$ has a longer (and therefore weaker) hydrogen bond than β-$(Ala)_n$: 1.86 Å[6] compared to 1.76 Å.[25] Our vibrational analysis also shows that the *f*(H···O) force constant is, as expected, smaller in α-$(Ala)_n$ than in β-$(Ala)_n$: 0.120 compared to 0.150 (see Table I). The decrease in frequency on cooling, viz., from 3279 to 3250 cm^{-1}, most likely arises from the shortening of the hydrogen bond that results from the contraction of the helix.

(b) C–H Stretching Region. The IR spectrum of the C–H stretching region is also shown in Figure 2. The Raman spectrum of this region, at the same two temperatures, is given in Figure 3. The assignments of the main band positions are straightforward and agree with those from β-$(Ala)_n$.[2]

Although band positions are similar, α-$(Ala)_n$ seems to exhibit a larger splitting between IR and Raman active components than does β-$(Ala)_n$ and also shows a distinct splitting of the ~2930-cm^{-1} band that is not present in the β structure. The latter splitting is temperature dependent: in the IR spectrum a singlet is observed at 2930 cm^{-1} at 373 K, which is the same frequency as in β-$(Ala)_n$ at room temperature; a doublet at 2925 and 2939 cm^{-1} is observed at 300 K, the higher frequency component being more intense; and at 120 K the splitting increases by 3–4 cm^{-1}, and the lower frequency component becomes more intense. This splitting, and its increase at low temperaure, it also observed in the Raman spectrum (cf. Figure 3). These effects are probably due to $CH_3 \cdots CH_3$ interactions in the crystal, a factor that was not included in our single-chain calculation of α-$(Ala)_n$, nor in our sheet calculation of β-$(Ala)_n$.[2]

A weak band is observed in this region at 2815 cm^{-1}. It has been shown[7] to have parallel dichroism, and we have observed that it disappears on *N*-deuteration. It also shifts to higher frequency on cooling, similar to the observed shift of the amide II band at 1545 cm^{-1} (cf. Table IV). It is very likely that this band arises from an amide II + amide III combination: 1545

Table II
Observed and Calculated Frequencies (in cm^{-1}) of α-Helical Poly(L-alanine)

Frequencies					
Obsd		Calcd			
Raman	IR	A	E_1	E_2	Potential energy distribution[a]
	3279$_{\parallel}$[b]	3279	3279	3279	NH str (97)
2988	2983$_{\parallel}$	2984	2984	2984	CH_3 asym str 2 (99)
		2983	2983	2983	CH_3 asym str 1 (100)
2942	2939$_{\perp}$		2929		CH_3 sym str (96)
2930	2925$_{\parallel}$	2929		2929	CH_3 sym sr (96)
2880	2883$_{\parallel,\perp}$	2883	2883	2883	$C^{\alpha}H^{\alpha}$ str (98)
	2815$_{\parallel}$				1545 + 1270 = 2815
1655	1658$_{\parallel}$	1659			C=O str (75), $C^{\alpha}CN$ def (12)
			1663		C=O str (72), CN str (14), $C^{\alpha}CN$ def (13)
				1650	C=O str (76), $C^{\alpha}CN$ def (13), CN str (12)
				1546	NH ipb (66), CN str (19)
1543	1545$_{\perp}$		1543		NH ipb (64), CN str (22)
	1516	1520			NH ipb (59), CN str (27)
1458	1458$_{\parallel,\perp}$	1449	1449	1450	CH_3 asym bend 1 (61), CH_3 asym bend 2 (27)
		1448	1448	1448	CH_3 asym bend 2 (58), CH_3 asym bend 1 (26)
1397					?
1377	1381$_{\perp}$	1363	1363	1363	CH_3 sym bend (68), H^{α} bend 1 (12)
				1346	$C^{\alpha}C$ str (25), H^{α} bend 1 (25), NH ipb (15), H^{α} bend 2 (11)
1338			1340		$C^{\alpha}C$ str (23), H^{α} bend 1 (22), NH ipb (14), H^{α} bend 2 (14)
1326	1328$_{\parallel}$	1319			CH_3 sym bend (29), H^{α} bend 1 (27), $C^{\alpha}C$ str (15)
		1313			H^{α} bend 2 (36), NH ipb (17), CH_3 sym bend (15)
1308	1307$_{\parallel,\perp}$		1301		H^{α} bend 2 (52), CH_3 sym bend (15)
				1296	H^{α} bend 2 (51), CH_3 sym bend (19), H^{α} bend 1 (15), NC^{α} str (10)
1278				1287	H^{α} bend 2 (27), H^{α} bend 1 (11), NH ipb (10), NC^{α} str (10)
1271	1270$_{\perp}$		1278		H^{α} bend 2 (24), H^{α} bend 1 (22)
1261	1265	1270			H^{α} bend 1 (35), H^{α} bend 2 (19), NH ipb (11)
			1176		NC^{α} str (37), H^{α} bend 1 (16)
1167	1170$_{\parallel,\perp}$			1174	NC^{α} str (33), H^{α} bend 1 (26)
		1173			NC^{α} str (46), $C^{\alpha}C$ str (18), CH_3 rock 1 (13)
				1107	$C^{\alpha}C^{\beta}$ str (49), CH_3 rock 2 (18)
1105	1108$_{\perp}$		1107		$C^{\alpha}C^{\beta}$ str (52), CH_3 rock 2 (19)
		1107			$C^{\alpha}C^{\beta}$ str (58), CH_3 rock 2 (21)
1070					?
				1046	CH_3 rock 1 (59)
1050	1051$_{\perp}$		1038		CH_3 rock 1 (54)
1017	1016$_{\parallel}$	1022			CH_3 rock 1 (39), H^{α} bend 1 (20), $C^{\alpha}C^{\beta}$ str (14)
970	968$_{\parallel}$	977			CH_3 rock 2 (33), NC^{α} str (24), CH_3 rock 1 (22), $C^{\alpha}C$ str (12)
			965		CH_3 rock 2 (41), NC^{α} str (15)
940?				957	CH_3 rock 2 (48), NC^{α} str (13), H^{α} bend 1 (16)
929					?
908	909$_{\parallel}$	910			CN str (25), CNC^{α} def (19), C=O str (14)
				902	$C^{\alpha}C^{\beta}$ str (25), CN str (20), $C^{\alpha}C$ str (11)
882	893$_{\perp}$		899		CN str (22), $C^{\alpha}C^{\beta}$ str (15), CNC^{α} def (11)
773	774		782		CO opb (34), $NC^{\alpha}C$ def (12)
				766	CO opb (49), $NC^{\alpha}C$ def (13)
756		763			CO opb (19), CN tor (11), $NC^{\alpha}C$ def (10)
693	691$_{\parallel}$	701			C^{β} bend 1 (23), CO opb (22), CN tor (21), $C^{\alpha}CN$ def (18)
				673	CN tor (31), CO ipb (18), $C^{\alpha}C$ str (15)
662	658$_{\perp}$		660		CN tor (26), NH opb (16), CO opb (11), C^{β} bend 1 (10), $C^{\alpha}C$ str (10)
				639	NH opb (52), CN tor (49)
	618$_{\perp}$		628		CN tor (46), NH opb (40), CO opb (13)
	600	609			CN tor (51), NH opb (46), CO opb (19)
		559			CO ipb (28), NH opb (22), CO opb (12), C^{β} bend 2 (12), $C^{\alpha}CN$ def (11)
530	526$_{\perp}$		527		C^{β} bend 1 (27), CO ipb (13), $C^{\alpha}C$ str (10)
				503	C^{β} bend 1 (27), CO ipb (14), $C^{\alpha}C$ str (10)
375	375$_{\perp}$		382		CO ipb (18), NH opb (14), CNC^{α} def (10), $NC^{\alpha}C$ def (11)
				370	C^{β} bend 2 (31), $NC^{\alpha}C$ def (21), $C^{\alpha}CN$ def (13)
	~366	362			$NC^{\alpha}C$ def (24), C^{β} bend 2 (22), CO opb (14)
328	324$_{\perp}$		315		C^{β} bend 2 (52), $NC^{\alpha}C$ def (11)
310				310	CNC^{α} def (27), CO opb (18), CO ipb (18), C^{β} bend 1 (16)
294	290$_{\parallel}$	306			CO ipb (25), C^{β} bend 2 (22), CNC^{α} def (21)
260	259	256			$C^{\alpha}C^{\beta}$ tor (43), C^{β} bend 2 (22)
	240		244		$C^{\alpha}C^{\beta}$ tor (88)
				243	$C^{\alpha}C^{\beta}$ tor (94)
	223	228			$C^{\alpha}C^{\beta}$ tor (53), C^{β} bend 2 (14)
209?				203	C^{β} bend 2 (40), $C^{\alpha}CN$ def (22), CO opb (12), $NC^{\alpha}C$ def (12)
189	188$_{\perp}$		197		$NC^{\alpha}C$ def (13), CO opb (12), C^{β} bend 2 (11), $C^{\alpha}CN$ def (11)
165	163$_{\perp}$		161		CNC^{α} def (23), $C^{\alpha}CN$ def (18), C^{β} bend 1 (17), $NC^{\alpha}C$ def (15), NH opb (11)
159				155	NH opb (41), $NC^{\alpha}C$ def (11), C^{β} bend 1 (11)
	120$_{\parallel}$	139			CNC^{α} def (26), C^{β} bend 1 (25), $C^{\alpha}CN$ def (21), $NC^{\alpha}C$ def (10)

Table II (*continued*)

Frequencies					Potential energy distribution[a]
Obsd		Calcd			
Raman	IR	A	E_1	E_2	
	113$_\perp$		100		$C^\alpha C$ tor (31), NC^α tor (26), NH opb (14)
87	84	89			$C^\alpha C$ tor (36), NC^α tor (33)
				88	NH opb (20), CNC^α def (20), $NC^\alpha C$ def (16), C^β bend 1 (11)
				51	$C^\alpha C$ tor (45), NC^α tor (24), NH opb (11)
				42	H · · · O str (41), $C^\alpha C$ tor (27), NC^α tor (13)
	46		30		NH opb (30), $C^\alpha C$ tor (20), H · · · O str (19), $NC^\alpha C$ def (14), C^β bend 1 (11)

[a] Only contributions greater than 10% are included. [b] Unperturbed frequency.

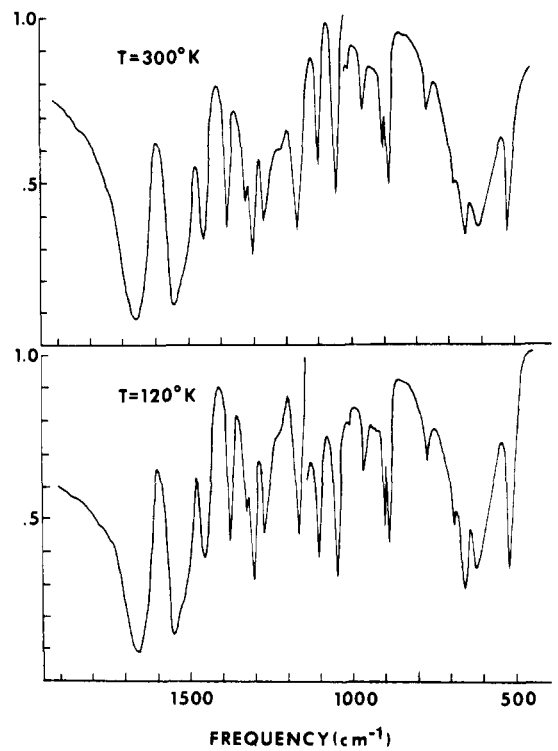

Figure 4. Infrared spectra of α-poly(L-alanine) in 1700–500-cm^{-1} region, at 300 and 120 K.

(E_1) + 1270 (E_1) = 2815 (A). We have observed that the 2780-cm^{-1} perpendicular IR band of β-(Ala)$_n$ mentioned by Elliott[7] exhibits the same low-temperature and *N*-deuteration behavior. It can also be accounted for by a similar combination: 1538 (A) + 1241 (B_2) = 2779 (B_2),[2] which seems to be prevalent in general in the IR spectra of β-polypeptides.[1]

(c) The 1700–500-cm^{-1} Region. Some IR bands in this region of the spectrum, which is shown in Figure 4, exhibit variations in band frequency and intensity with temperature, and therefore may be good indicators of how the structure changes with temperature. This will be discussed below in greater detail. The Raman spectrum, shown in Figure 5, also has some bands that vary with temperature.

The amide I and amide II modes are well accounted for by the calculation, which, as we have noted, includes transition dipole coupling contributions. The IR spectrum shows definite evidence only for the A species amide I mode, and we have therefore been unable to verify the predicted 13-cm^{-1} splitting between E_1 and E_2 species modes. The splitting between A and E_1 species amide II modes is very well reproduced by the calculations.

It should be noted that we find (see Table I) that f(C=O) in α-(Ala)$_n$ is slightly lower than that in β-(Ala)$_n$. As we remarked earlier, the hydrogen bond in the former structure is longer than that in the latter, and this implies a weaker hydrogen bond in α-(Ala)$_n$, which is supported by the higher f(N–H) and the lower f(H· · · O) force constants. It might be expected, therefore, that f(C=O) in α-(Ala)$_n$ should also be higher, contrary to our findings. Our calculations show, however, that the C=O stretching frequency (amide I) is totally independent of the hydrogen bond strength as reflected by the values of f(N–H) and f(H· · ·O). It may, therefore, be necessary to re-introduce the f(C=O, H· · ·O) interaction constant used earlier[26,27] if an adequate description of the influence of hydrogen bonding on f(C=O) is to be obtained (the amide I frequency is influenced significantly by this force constant).

The CH_3 asymmetric bend and the CH_3 symmetric bend modes are only moderately well predicted. In the latter case the Raman band seems to be split in high molecular weight α-(Ala)$_n$, with components at 1377 and 1384 cm^{-1}; this may be a result of interchain interactions. It is certainly possible to make changes in the force constants associated with the alanyl residue that would enhance the agreement between observed and calculated CH_3 bending modes. However, our motivation for doing normal vibration calculations on α-(Ala)$_n$ is to develop a single force field which is transferable to both the helical and extended polypeptide chain structures. The fact that the predictions for methyl bending frequencies are good for the β form of (Ala)$_n$ and only fair for the α-helical form is significant. In this region of the IR spectrum of β-(Ala)$_n$ the bending of H^α, N–H in-plane bend, and CH_3 bend contribute. However, in the α helix the contribution from NH

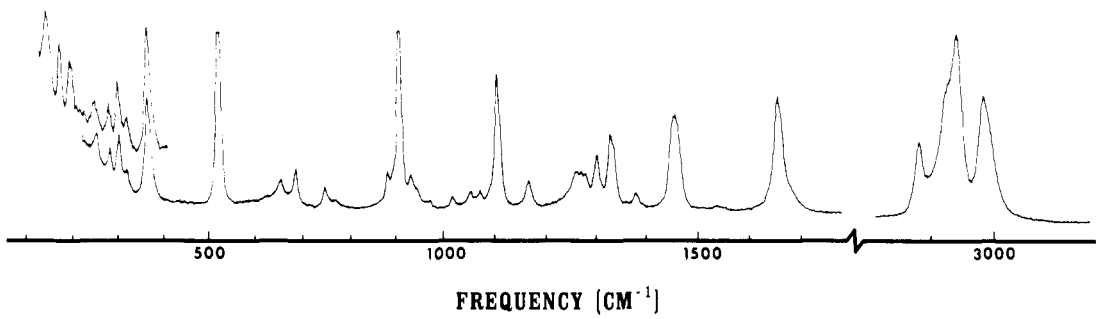

Figure 5. Raman spectrum of α-poly(L-alanine) in 1700–100-cm^{-1} region.

Table III
Observed and Calculated Frequencies (in cm^{-1}) of α-Helical Poly(L-alanine-*N*-*d*)

Frequencies					
Obsd		Calcd			
Raman	IR	A	E_1	E_2	Potential energy distribution[a]
2988	2982	2984	2984	2984	CH_3 asym str 2 (99)
		2983	2983	2983	CH_3 asym str 1 (100)
2940	2941	2929			CH_3 sym str (99)
	2924		2929	2929	CH_3 sym str (95)
2886	2879	2883	2883	2883	$C^\alpha H^\alpha$ str (99)
	2441[b]	2410			ND str (96)
			2409	2413	ND str (95)
	1650	1647			C=O str (80), CN str (12), $C^\alpha CN$ def (12)
1652			1656		C=O str (78), CN str (12), $C^\alpha CN$ def (12)
				1647	C=O str (79), CN str (12), $C^\alpha CN$ def (12)
1477	1470	1458			CH_3 asym bend 2 (33), CN str (18), CO ipb (10), $C^\alpha C$ str (10)
			1457	1457	CH_3 asym bend 1 (32), CH_3 asym bend 2 (16), CN str (15), $C^\alpha C$ str (11)
1455	1454	1449			CH_3 asym bend 1 (71), CH_3 asym bend 2 (16)
			1449		CH_3 asym bend 2 (55), CH_3 asym bend 1 (31)
				1449	CH_3 asym bend 1 (83)
	1439	1436			CH_3 asym bend 2 (38), CN str (20), CH_3 asym bend 1 (10)
			1434		CH_3 asym bend 1 (24), CN str (23), CH_3 asym bend 2 (14), $C^\alpha C$ str (12), $C^\alpha CN$ def (12)
~1430				1433	CH_3 asym bend 1 (34), CN str (24), CO ipb (13), $C^\alpha C$ str (12), $C^\alpha CN$ def (12)
				1361	CH_3 bend (73), H^α bend 1 (12)
		1360			CH_3 sym bend (77), H^α bend 1 (10)
1373	1379		1360		CH_3 sym bend (75), H^α bend 1 (11)
				1320	H^α bend 2 (33), H^α bend 1 (28)
			1318		H^α bend 2 (41), H^α bend 1 (27)
1326	1328	1316			H^α bend 2 (54), H^α bend 1 (25)
				1292	H^α bend 2 (53), CH_3 sym bend (19), H^α bend 1 (17)
			1288		H^α bend 2 (45), H^α bend 1 (24), CH_3 sym bend (20)
1296	1293	1282			H^α bend 1 (37), H^α bend 2 (33), CH_3 sym bend (20)
1244					?
				1178	NC^α str (36), H^α bend 1 (21)
	1178		1175		NC^α str (39), H^α bend 1 (14)
	1170	1171			NC^α str (44), $C^\alpha C$ str (19), CH_3 rock 1 (14)
1158					?
	1140				?
				1134	$C^\alpha C^\beta$ str (44), ND ipb (16), CH_3 rock 2 (13)
			1127		$C^\alpha C^\beta$ str (44), CH_3 rock 2 (18), ND ipb (13)
1095	1098	1111			$C^\alpha C^\beta$ str (48), CH_3 rock 2 (25)
				1067	CH_3 rock 1 (52), ND ipb (14)
1065	1062		1061		CH_3 rock 1 (39), ND ipb (18), H^α bend 1 (11), $C^\alpha C^\beta$ str (10)
		1052			ND ipb (32), $C^\alpha C^\beta$ str (21), H^α bend 1 (16)
	1015	1005			CH_3 rock 1 (53), ND ipb (21)
1001	999		992		ND ipb (41), CH_3 rock 1 (26)
				988	ND ipb (43), CH_3 rock 1 (16), CH_3 rock 2 (15)
975	974		956		CH_3 rock 2 (43), NC^α str (15)
945	944	953			CH_3 rock 2 (35), ND ipb (21), NC^α str (17)
				949	CH_3 rock 2 (40), NC^α str (14), H^α bend 2 (10)
893	887	892			CN str (26), CO ipb (20), C=O str (14)
				890	CN str (27), $C^\alpha C^\beta$ str (20), $C^\alpha C$ str (11)
	880		884		CN str (27), CNC^α def (12), $C^\alpha C^\beta$ str (12)
839					?
755	762		763		CO opb (38), C^β bend 1 (12)
				756	CO opb (49), C^β bend 1 (12)
		733			CO opb (19), $NC^\alpha C$ def (12), C^β bend 1 (12), $C^\alpha CN$ def (11)
682	680	687			CO opb (42), C^α bend 1 (20), $C^\alpha CN$ def (13)
660				658	CO ipb (26), $C^\alpha C$ str (21)
	647		645		CO opb (19), CO ipb (16), $C^\alpha CN$ def (15), $C^\alpha C$ str (13)
	595?	567			CO ipb (26), $C^\alpha C$ str (16), NC^α str (10)
522	523		535		$NC^\alpha C$ def (24), ND opb (14), CO ipb (13)
				505	$NC^\alpha C$ def (25), ND opb (23), CN tor (13)
				484	CN tor (54), ND opb (30), CO ipb (10)
	458		472		CN tor (67), ND opb (39)
		465			ND opb (75), CN tor (66), CO opb (10)

Table III (*continued*)

Frequencies					
Obsd		Calcd			
Raman	IR	A	E_1	E_2	Potential energy distribution[a]
374		376			CO ipb (19), ND opb (15), CNC$^\alpha$ def (11), C$^\beta$ bend 1 (11), CN tor (11)
				365	C$^\beta$ bend 2 (28), C$^\beta$ bend 1 (24), CN tor (12), CO ipb (10)
363		360			C$^\beta$ bend 1 (22), C$^\beta$ bend 2 (19), CO opb (12)
301			309		C$^\beta$ bend 2 (56), ND opb (13), C$^\beta$ bend 1 (10)
		298			C$^\beta$ bend 2 (32), CO ipb (23), CNC$^\alpha$ def (18), CN tor (14)
				298	CNC$^\alpha$ def (25), NC$^\alpha$C def (18), ND opb (16), CO opb (15), CO ipb (15), CN tor (12)
		254			C$^\alpha$C$^\beta$ tor (50), C$^\beta$ bend 2 (16)
			244		C$^\alpha$C$^\beta$ tor (89)
				242	C$^\alpha$C$^\beta$ tor (94)
		226			C$^\alpha$C$^\beta$ tor (46), C$^\beta$ bend 2 (14)
				203	C$^\beta$ bend 2 (40), C$^\alpha$CN def (22), C$^\beta$ bend 1 (12), CO opb (12)
			194		C$^\beta$ bend 1 (13), C$^\beta$ bend 2 (11), CO opb (11), C$^\alpha$CN def (11)
			160		CNC$^\alpha$ def (24), C$^\alpha$CN def (17), NC$^\alpha$C def (17), C$^\beta$ bend 1 (14), ND opb (11)
				153	ND opb (36), C$^\beta$ bend 1 (11), NC$^\alpha$C def (10)
		139			CNC$^\alpha$ def (26), NC$^\alpha$C def (25), C$^\alpha$CN def (21)
			99		C$^\alpha$C tor (31), NC$^\alpha$ tor (26), ND opb (13)
		88			C$^\alpha$C tor (36), NC$^\alpha$ tor (34)
				88	ND opb (20), CNC$^\alpha$ def (20), C$^\alpha$C tor (13), NC$^\alpha$C def (11)
				51	C$^\alpha$C tor (44), NC$^\alpha$ tor (25), ND opb (10)
				41	D$\cdots$O str (40), C$^\alpha$C tor (28), NC$^\alpha$ tor (12)
			30		ND opb (30), C$^\alpha$C tor (21), D$\cdots$O str (15), C$^\beta$ bend 1 (13), NC$^\alpha$C def (11)

[a] Only contributions greater than 10% are included. [b] Unperturbed frequency.

Table IV
Fermi Resonance Calculations of Unperturbed N–H and N–D Stretching and of Amide II and Amide II′ + Amide III′ Frequencies (in cm^{-1}) in α-Poly(L-alanine) and α-Poly(L-alanine-*N*-*d*)

	Obsd			Calcd		
	Frequency		Intensity			
Temp, K	ν_a	ν_b	I_R	ν_a^0	ν_b^0	Amide II
α-(Ala)$_n$						
300		3307	3058	0.127	3279	3086	1543 [obsd 1545]
120		3286	3070	0.200	3250	3106	1553 [obsd 1553]
α-(Ala-N-d)$_n$						Amide II′ + amide III′
300		2464	2407	0.68	2441	2430	1439 (E_1) + 999 (E_1) = 2438 (A)
120		2462	2403	0.99	2433	2432	1444 (E_1) + 999 (E_1) = 2443 (A)

in-plane bend is not significant. Therefore, although we are confident of the assignments of the methyl bending modes in both forms, small changes in force constants will result from further refinement. Such a refinement will be less meaningful without data from observed spectra of other polypeptides in the α-helical form.

Several weak bands have been observed in the 1360–1400-cm^{-1} region, the assignments of which still seem to be in question.[17,19] We find two weak bands at 1377 and 1397 cm^{-1} in the Raman spectrum (see Figure 5), the former shifting to 1373 cm^{-1} on *N*-deuteration. Our calculated CH_3 symmetric bend mode, at 1363 cm^{-1}, is predicted to shift by 3 cm^{-1} on *N*-deuteration, which corresponds well with the observed Raman (4 cm^{-1}) and IR (3 cm^{-1}) shifts. We therefore assign the 1377-cm^{-1} band to CH_3 symmetric bend, leaving the 1397-cm^{-1} band unassigned to a fundamental mode.

The A species H$^\alpha$ bend mode near 1328 cm^{-1} is very well accounted for by the calculation. At −150 °C it splits, with a second band appearing at 1338 cm^{-1}. Perhaps this is the E_1 mode that we calculate at 1340 cm^{-1}. The 1307 cm^{-1} parallel IR band, located at 1308 cm^{-1} in the Raman, can be confidently assigned to the A species mode calculated at 1313 cm^{-1}, which is mainly H$^\alpha$ bend 2 plus some NH in-plane bend. This assignment gains support from the observed shift of this band to 1293 cm^{-1} (predicted at 1282 cm^{-1}) on *N*-deuteration (see below).

Three Raman bands are observed at 1261, 1271, and 1278 cm^{-1} in the amide III region. Based on polarization data,[10] these bands have been assigned to A, E_1, and E_2 species, respectively.[16] Our calculated amide III modes correspond well to the progression and symmetry designations of the assigned frequencies. As expected, these bands disappear on *N*-deuteration.

The skeletal stretching and CH_3 rocking modes in the 1100–900-cm^{-1} region can be satisfactorily assigned from the calculation, although the agreement is only fair in some cases. A Raman band at 1070 cm^{-1} may be associated with β-(Ala)$_n$, although the absence of a comparable band near 1235 cm^{-1} makes this assignment unlikely. It is perhaps possible that the 1070-cm^{-1} band should be assigned to the E_2 species CH_3 rock calculated at 1046 cm^{-1}, the poor agreement being attributable to the presence of the $CH_3\cdots CH_3$ interactions mentioned earlier.

The band near 1017 cm^{-1} can be correlated with short chain segments, since it is observed in the Raman spectra of L-Ala oligomers up to the pentamer.[13] It does, however, correspond well to the calculated frequency at 1022 cm^{-1}. The weak Raman band at 929 cm^{-1} is not assignable to a fundamental mode of vibration.

The 618-cm^{-1} perpendicular IR band is satisfactorily assigned to the E_1 species mode at 628 cm^{-1}. The contribution of NH out-of-plane bend to this mode would account for its shift on *N*-deuteration. The characteristic α-helix band near 525–530 cm^{-1} is very well predicted by the calculation and is an important criterion supporting the transferability of this force field from the β-polypeptides.

(d) Low-Frequency Region. Far-IR spectra of α-(Ala)$_n$ are shown in Figure 6. The strong bands at 375, 324, and 290

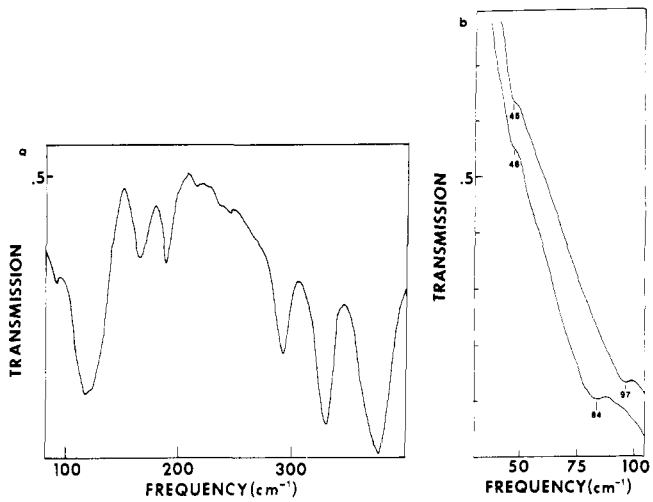

Figure 6. Far-infrared spectra of α-poly(L-alanine): (a) 400–100-cm^{-1} region; (b) 100–25-cm^{-1} region.

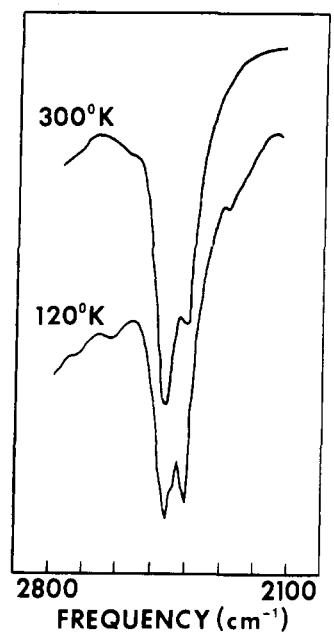

Figure 7. Infrared spectra of α-poly(L-alanine-*N*-*d*) in the N–D stretching region, at 300 and 120 K.

cm^{-1} are well accounted for by the calculations, although the frequency agreement is only fair for the last band. Weak bands at 259, 240, and 223 cm^{-1} agree well with the predicted CH_3 torsion modes calculated in this region. It is interesting that the calculated (and presumably observed) spread in these modes for α-$(Ala)_n$, viz., 28 cm^{-1}, is very large in comparison to that for β-$(Ala)_n$, where essentially no splitting is predicted.[2] This contrasts with the observation from inelastic neutron scattering,[28] which indicates that both α and β structures give a peak in the spectrum at about 230 cm^{-1}. The inelastic neutron scattering spectrum, of course, reflects the density of states, which may not be as sensitive to chain conformation as are the optically active modes.

The bands below 200 cm^{-1} are reasonably well reproduced, although some eventual force constant refinement may be desirable for this region. The force constants for N–C^α and C^α–C torsions have been greatly increased, from 0.037 to 0.110. (This is not necessarily surprising, since these torsion force constants could be expected to depend on the respective values of the ϕ and ψ torsion angles.) Below 200 cm^{-1}, six IR bands are observed (188, 163, 120, 113, 84, 46 cm^{-1}) and six are predicted. The assignments of the three higher frequency bands are consistent with dichroic data. The predicted frequencies of the bands observed at 113, 84, and 46 cm^{-1} are almost totally dependent on torsion force constants. With $f(\tau) = 0.037$ we predict a band with A symmetry at 60 cm^{-1} and two with E_1 symmetry at 73 and 26 cm^{-1}, and with $f(\tau) = 0.110$ the three frequencies are calculated at 89, 100, and 30 cm^{-1}, respectively. Although agreement is only fair, we believe the assignment is correct.

(2) α-Poly(L-alanine-*N*-*d*). (a) C–H Stretching Region. Similar bands are predicted in this region for the deuterated as for the normal polypeptide. The 2941, 2924 cm^{-1} IR doublet for CH_3 symmetric stretch in α-(Ala-*N*-*d*), analogous to the 2939, 2925 cm^{-1} pair in α-$(Ala)_n$, may again be a result of $CH_3 \cdots CH_3$ interchain interactions.

(b) N–D Stretching Region. On replacing N–H by N–D, the amide A and B bands disappear and two new bands appear in the IR at 2407 and 2464 cm^{-1} at 300 K. On cooling to 120 K these bands shift to 2403 and 2462 cm^{-1}, their relative intensity changes, and a weak band appears at 2450 cm^{-1} (see Figure 7). The main doublet has been attributed[29] to a Fermi resonance between N–D stretching and a combination of amide II′ and amide III′.

Using the observed intensity ratios for the components of the doublet (see Table IV), and doing a Fermi resonance analysis similar to that for N–H, we find that the unperturbed N–D stretching frequency is at 2441 cm^{-1} at 300 K and at 2433 cm^{-1} at 120 K. The unperturbed ν_b^0 band, at 2430 cm^{-1} at 300 K and 2432 cm^{-1} at 120 K, agrees well with the amide II′ + amide III′ combination, a combination which we have already seen is present in the undeuterated molecule. The decrease in the N–D stretching frequency on cooling to 120 K is consistent with a contraction of the helix. The slight increase in ν_b^0 on cooling agrees with our observed increase in amide II′ (from 1439 to 1444 cm^{-1}), since the amide III′ mode is essentially unaffected.

The calculated N–D stretching frequency, using the value of f(N–H) in the normal vibration calculation, is seen to be low by 31 cm^{-1}. It would be necessary to increase f(N–D) by 0.160 to bring the calculated frequency into agreement with the observed. There are at least two reasons why an increase in this force constant would be expected. First, the hydrogen bond in a deuterated α helix is known to be slightly longer, and therefore weaker, than that in the undeuterated helix.[21] As a consequence, f(N–D) should be larger than f(N–H). Second, since anharmonicities for H stretching modes are larger than for D stretching modes, and are in general negative,[30] our harmonic force field overcompensates by assigning a smaller force constant to N–H stretch than is appropriate for N–D stretch. Further study will be needed to show whether the required increase of 0.160 is consistent with these two factors.

(c) The 1700–300-cm^{-1} Region[1]. The amide I′ band is observed to shift down by 3 cm^{-1} (Raman) to 8 cm^{-1} (IR) as a result of *N*-deuteration. The calculation predicts a downward shift of this mode of 7 to 12 cm^{-1}, in fair agreement with observation.

The assignment of the amide II′ mode needs to be considered with some care. As α-$(Ala)_n$ is progressively deuterated (see Figure 8), a new band appears at 1439 cm^{-1}. At the same time the single CH_3 asymmetric bend mode at 1458 cm^{-1} is replaced by two bands at 1454 and 1470 cm^{-1}. These two bands are also seen in the Raman spectrum,[17,19] and a weak shoulder is observed[17] near 1430 cm^{-1}. The 1454-cm^{-1} band clearly derives from the strong 1458-cm^{-1} CH_3 asymmetric bend mode of α-$(Ala)_n$, and we suggest that the ~1470-cm^{-1} band is probably also such a mode. The strong IR band at 1439 cm^{-1} (weak in the Raman) should therefore be related to

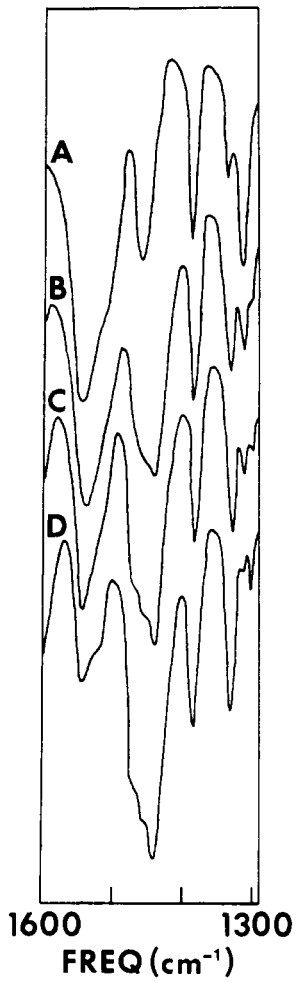

Figure 8. Infrared spectra of (A) α-poly(L-alanine) and (B–D) progressively deuterated samples, in the 1600–1300-cm^{-1} region.

amide II′, which would be consistent with the observation of strong IR bands at 1445 cm^{-1} in *N*-deuterated α-poly(γ-benzyl L-glutamate),[21] at 1455 cm^{-1} in *N*-deuterated α-poly(β-benzyl L-apartate),[21] and at 1437 cm^{-1} in *N*-deuterated α-keratin.[31] If the splitting of the doubly degenerate CH_3 asymmetric bend mode of α-$(Ala)_n$ (which is also calculated to be essentially degenerate, as is evident from Table II) occurs as we suggest, it probably arises from a resonance of one component of this mode with the amide II′ mode, the perturbed modes being located at 1470 and 1439 cm^{-1} in the IR. This implies that the "unperturbed" amide II′ mode is probably located near 1439 + (1470–1458) = 1451 cm^{-1}.

Our previous force field[1,2] led to a calculated amide II′ mode at 1469 cm^{-1}, whose potential energy distribution was CN str (31), $C^{\alpha}C$ str (17), ND ipb (11), CH_3 asym bend 2 (10). In view of the above analysis, we have decided to change *f*(C–N), and consequently *f*(C=O), to give an amide II′ frequency close to 1451 cm^{-1}. The required change of 0.500 in *f*(C–N) (indicated by the Jacobian matrix element) is within the uncertainty associated with this force constant.[26] When the new force constants were used, a considerably different mixing occurred between the CH_3 asymmetric bend and amide II′, and the three bands were now predicted at 1458, 1449 (unchanged), and 1436 cm^{-1}. While the latter mode was previously calculated at 1443 cm^{-1}, and had no CN str component, it is now seen to have the largest such amide II′ contribution. Again if we recall that the CH_3 bend modes are predicted rather low, the assignments in Table III are most probably correct. While we feel that it is not unreasonable to expect that such resonance may occur in this region of the spectra of polypeptides, the specific details will have to await a joint study of β and α structures.

Progressive deuteration of α-$(Ala)_n$ results in other significant changes in band intensities in this region: the 1307-cm^{-1} band decreases in intensity and increased intensity appears at 1328 and 1293 cm^{-1} (see Figure 8). The normal vibration analyses clearly show the reason for this: the mode at 1328 cm^{-1} has changed character from α-$(Ala)_n$ to α-$(Ala\text{-}N\text{-}d)_n$. As we noted earlier, the 1307-cm^{-1} band in α-$(Ala)_n$ is assignable to a mode containing N–H in-plane bend, and this contribution will therefore disappear on *N*-deuteration. When this happens, the H^{α} bend 1 and H^{α} bend 2 contributions redistribute themselves: in α-$(Ala)_n$ the 1307-cm^{-1} band contains H^{α} bend 2 and the 1328-cm^{-1} band contains H^{α} bend 1, whereas in α-$(Ala\text{-}N\text{-}d)_n$ the H^{α} bend 2 component has moved to the 1328-cm^{-1} band and the larger H^{α} bend 1 component is at 1293 cm^{-1}. Since in α-$(Ala)_n$ the intensity seems to be associated with the H^{α} bend 2 component, it is not surprising that the 1328-cm^{-1} band is enhanced in intensity in α-$(Ala\text{-}N\text{-}d)_n$.

The bands in the 1100–1200-cm^{-1} region are moderately well accounted for. The weak band at 1095 cm^{-1} in the Raman is not nearly as well predicted as its strong counterpart in α-$(Ala)_n$ at 1105 cm^{-1}. Perhaps the decrease in intensity is related to the admixture of N–D in-plane bend for the α-$(Ala\text{-}N\text{-}d)_n$ mode. The main N–D in-plane bend mode at 1000 cm^{-1} is well predicted. The presumably large observed split-

Table V
Variation of Frequency with Helix Geometry for Poly(L-Alanine)

Obsd freq for *T* =			Calcd freq for *h*, *t*, and χ_1 =			
			1.495 Å, 99.57°, 0°	1.495 Å 99.57°, 20°	1.474 Å, 99.57°, 0°	1.474 Å, 98.57°, 0°
150 °C	23 °C	−150 °C				
1303	1307	1309	1313	1314	1313	1313
1104	1108	1110	1107	1103	1106	1107
	1105	1110				
688	691	694	701	702	704	704
	693	695				
655	658	660	660	660	662	661
604	618	625	628	628	631	626
	324	326	315	315	315	315
	290	294	306	307	304	305
	188	192	197	198	199	197
	115[a]	122	139	139	141	140
			100	94	103	101

[a] Measured as a single band in ref 18.

ting of CH_3 rock modes at 975 and 945 cm^{-1} is poorly accounted for. This may be related to deficiencies in the CH_3 force field, as discussed earlier. The strong Raman band at 893 cm^{-1} is very well accounted for, as was its counterpart (of similar potential energy distribution) at 908 cm^{-} in α-$(Ala)_n$. The remaining observed bands, down to 300 cm^{-1}, are fairly well predicted. Data below this region were not available.

(3) Variation of Frequency with Structure. As we noted earlier, some bands in the spectrum of α-$(Ala)_n$ are affected in intensity and position by change in temperature. Bands in the IR at 324, 290, 188, and 115 cm^{-1} were found[18] to shift by 3–5 cm^{-1} on cooling to low temperatures. In our study of other bands in the spectrum we have observed that IR bands at 1307, 1108, 691, 658, and 618 cm^{-1} and Raman bands at 1105 and 693 cm^{-1} are similarly affected in frequency and intensity by change in temperature (see Table V).

In an effort to determine the origin of a least the frequency shifts, we have calculated the influence of changes in geometry on the normal vibration frequencies. In these calculations the force field was kept constant and small changes were made in h, t, and χ_1. The effects of such changes on some of the calculated frequencies are shown in Table V. It should be kept in mind that the frequency shifts with temperature in the N–H stretching region have already shown that the hydrogen bond gets stronger at low temperature. We therefore expect that lower temperature will at least be associated with smaller values of h.

The first thing to note from these calculations is that changing χ_1 has relatively little effect on all frequencies except those at 1108 and possibly 115 cm^{-1}. The former mode, which contains CH_3 rock, increases in frequency as χ_1 is decreased from 20 to 0°. Since 20° is closer to the favored value, and since χ_1 tends to decrease with decreasing h (which would occur at the lower temperatures), this factor may play an important role in determining the frequency of this mode. The origin of the sensitivity of the 100-cm^{-1} (predicted) band to changes in χ_1 is less clear. Second, we see that modes at 691 and 618 cm^{-1} both increase in frequency as h is decreased, the former being relatively insensitive to changes in t while the latter is highly sensitive to such changes. Since the 691-cm^{-1} band is observed to change much less with temperature than does the 618-cm^{-1} band, it may be reasonable to suppose that both h and t are influenced by temperature changes, in turn affecting the vibrational frequencies. (If t is important, the calculations indicate that it increases as the temperature is lowered.) We should note that the changes we have made in h and t are quite small; these parameters may actually undergo larger changes with temperature.

If we try to assess whether there is a common origin to bands that shift with temperature, it is intriguing to observe that most bands have as components C^β bend (691, 324, 290, 188, and 115 cm^{-1}) and/or CO or NH out-of-plane bend (691, 658, 618, and 188 cm^{-1}). Since lowering the temperature undoubtedly causes lateral contraction of the lattice, which would enhance interchain interactions, it is possible that the initial influence is felt by the bending coordinates associated with the CH_3 group. This would imply that effective diagonal force constants associated with such bending coordinates (which are involved in the C^β bend coordinates) could increase as interchain interactions increase. In a similar vein, changes in t could be expected to alter force constants associated with CO and NH out-of-plane bending, thus influencing modes that contain these coordinates.

It is clear from the above discussion that changes in geometry, which are reasonable consequences of temperature changes, can influence the vibrational frequencies. If these are associated with (probably expected) changes in the force field, then the observed frequency shifts (and intensity changes) are not unreasonable. The situation is obviously complex; thus, low frequencies could shift as a result of a change in the population of excited levels. More work will be needed to clarify completely the factors involved.

Conclusions

It has been possible to show that the force field developed for the β-polypeptides[1,2] can be substantially transferred to the α-helical structure with minimal changes. Some of these have an obvious origin: (1) f(N–H) and f(H···O) change because of differences in hydrogen bond strength; (2) f(N–H op), and the associated f(N–H; op, $NC^\alpha C$) and f(N–H op, $NC^\alpha C^\beta$) as well as perhaps $f(C^\alpha$–N–H) and f(C–N–H), may differ because of the differing hydrogen bond structures in the two conformations; (3) $f(N–C^\alpha$ tor) and $f(C^\alpha$–C tor) are different probably because of different ϕ and ψ values (although there may now be a stronger basis for an improved refinement of this value). Other changes reflect the unrefined force constants associated with the CH_3 group, as we have noted earlier: these include $f(C^\alpha$–$C^\beta)$, $f(N–C^\alpha–C)$, and $f(C–N–C^\alpha)$. And finally, the changes in f(C–N) and f(C=O) are a result of our recognition that amide II′ must be reassigned.

It is evident from the above that, before we can be sure of which force constant changes are real, we must attempt a joint refinement of a common force field for α and β structures. This will be reported on in future publications. Nevertheless, at this stage a significant improvement has been achieved in analyzing the vibrational spectrum of the α helix, in particular by applying a force field that is substantially the same as that for β-polypeptides and, for the first time, including all atoms in the calculation. This approach has also enabled us to analyze changes in spectrum with temperature in terms of structural changes and to assess with reasonable confidence the significance of the various contributing factors.

Acknowledgment. This work was supported by National Science Foundation Grants CHE75-05239 and PCM76-83047.

References and Notes

(1) W. H. Moore and S. Krimm, *Biopolymers*, **15**, 2439 (1976).
(2) W. H. Moore and S. Krimm, *Biopolymers*, **15**, 2465 (1976).
(3) L. Brown and I. F. Trotter, *Trans. Faraday Soc.*, **52**, 537 (1956).
(4) A. Elliott and B. R. Malcolm, *Proc. R. Soc. London, Ser. A*, **249**, 30 (1959).
(5) S. Arnott and A. J. Wonacott, *J. Mol. Biol.* **21**, 371 (1966).
(6) S. Arnott and S. D. Dover, *J. Mol. Biol.*, **30**, 209 (1967).
(7) A. Elliott, *Proc. R. Soc. London, Ser. A*, **226**, 403 (1954).
(8) C. H. Bamford, A. Elliott, W. E. Hanby, "Synthetic Polypeptides", Academic Press, New York, N.Y., 1956.
(9) K. Itoh, T. Nakahara, T. Shimanouchi, M. Oya, K. Uno, and Y. Iwakura, *Biopolymers*, **6**, 1759 (1968).
(10) B. Fanconi, B. Tomlinson, L. Nafie, W. Small, and W. Peticolas, *J. Chem. Phys.*, **51**, 3993 (1969).
(11) K. Itoh, T. Shimanouchi, and M. Oya, *Biopolymers*, **7**, 649 (1969).
(12) K. Itoh and T. Shimanouchi, *Biopolymers*, **9**, 383 (1970).
(13) P. Sutton and J. L. Koenig, *Biopolymers*, **9**, 615 (1970).
(14) L. Simons, G. Bergström, G. Blomfelt, S. Forss, H. Stenbäck, and G. Wansén, *Commentat. Phys.-Math., Soc. Sci. Fenn.*, **42**, 125 (1972).
(15) B. Fanconi, *Biopolymers*, **12**, 2759 (1973).
(16) M. C. Chen and R. C. Lord, *J. Am. Chem. Soc.*, **96**, 4750 (1974).
(17) B. G. Frushour and J. L. Koenig, *Biopolymers*, **13**, 455 (1974).
(18) K. W. Johnson, K. Krishnan, and J. F. Rabolt, *Bull. Am. Phys. Soc.*, **20**, 372 (1975).
(19) B. Fanconi, E. Small, and W. Petccolas, *Biopolymers*, **10**, 1277 (1971).
(20) S. L. Hsu, W. H. Moore, and S. Krimm, *J. Appl. Phys.*, **46**, 4185 (1975).
(21) K. Tomita, A. Rich, C. deLozé, and E. R. Blout, *J. Mol. Biol.*, **4**, 83 (1962).
(22) Yu. N. Chirgadze and E. V. Brazhnikov, *Biopolymers*, **13**, 1701 (1974).
(23) Yu. N. Chirgadze, B. V. Shestopalov, and S. Y. Venyaminov, *Biopolymers*, **12**, 1337 (1973).
(24) T. Miyazawa, *J. Mol. Spectrosc.*, **4**, 168 (1960).
(25) S. Arnott, S. D. Dover, and A. Elliott, *J. Mol. Biol.*, **30**, 201 (1967).
(26) Y. Abe and S. Krimm, *Biopolymers*, **11**, 1817 (1972).
(27) S. Krimm and Y. Abe, *Proc. Natl. Acad. Sci. U.S.A.*, **69**, 2788 (1972).
(28) W. Drexel and W. Petricolas, *Biopolymers*, **14**, 715 (1975).
(29) C. G. Cannon, *Spectrochim. Acta*, **16**, 302 (1960).
(30) G. Herzberg, "Infrared and Raman Spectra", Van Nostrand, New York, N.Y., 1945.
(31) E. G. Bendit, *Biopolymers*, **4**, 561 (1966).